ISSN:3007-9640 DOI: https://doi.org/10.70114/acmsr.2025.3.1.P126

Elastic-Plastic Analysis of Seismic Performance for Bridges with Corrugated Steel Webs

Gang Wang [1, a], Lei Fan [1, b], Jianshe Liu [2, c], Kunning Zhu [3, d], Shuo Huang [2, e],

[1] Xuzhou Highway Development Center, China;

[2] CCCC Second Highway Engineering Bureau Co., Ltd, China;

[3] China Design Group, China.

[a] 35261832@qq.com, [b] 24883419@qq.com, [c] 467410881@qq.com, [d] redkun@163.com,

[e] 844491060@qq.com,

Abstract. This paper examines a corrugated steel web prestressed concrete (PC) continuous box girder bridge constructed in China. Finite element analysis was employed to simulate the structure, and the seismic response of the bridge was calculated using elastic time-history and elasto-plastic time-history analysis. The analysis results indicate that, when using a plastic hinge model to simulate the pier, the pier undergoes bending into a plastic state under E2 seismic conditions, reaching the first yield state longitudinally and exhibiting slight plasticity laterally. These findings provide technical support for the design and construction of similar bridges in the future.

Keywords: Corrugated steel web; Composite box girder; Seismic Analysis; Elastic time-history; Elasto-plastic time-history analysis.

1. Introduction

In composite bridges with corrugated steel webs, the traditional concrete webs are replaced with corrugated steel webs. This substitution offers advantages such as reduced self-weight and higher prestress efficiency, thereby optimizing material properties [1-3]. Regarding its dynamic characteristics, extensive research has been conducted by scholars through experiments and finite element simulations [4-5]. The time history analysis method is the primary approach for addressing structural dynamics problems [6]. Additionally, extensive research has been conducted by scholars on elasto-plastic time-history seismic analysis [7-8].

Fig. 1. Beijing-Hangzhou Grand Canal Bridge (Xuzhou Eastern Bypass Expressway)

However, stochastic seismic response analysis is not yet well-developed and requires further study before being implemented in engineering practice. In this paper, elastic time-history and elasto-plastic time-history seismic method are used to analyze the seismic response of the PC composite continuous box-girder bridge with corrugated steel webs.

2. Finite Element Modeling

This paper takes a PC composite box girder bridge with corrugated steel webs as the engineering background. The total length of the bridge is 764.28m. The main span is a pre-stressed concrete

ISSN:3007-9640 DOI: https://doi.org/10.70114/acmsr.2025.3.1.P126
continuous girder with corrugated steel webs, designed as fully pre-stressed components in the longitudinal direction. The main pier of main bridge is a solid pier, the transition pier has a column pier, and the foundation of the entire bridge is drilled cast-in-place pile foundations.

This paper simulates a corrugated web box-girder bridge using MIDAS Civil software. In the finite element bridge model, there are 84 elements and 93 nodes. When the bridge is modeled, the coordinate is defined as the x-direction along the bridge, the y-direction across the bridge, and the z-direction vertically. The finite element model is shown in Figure 2.

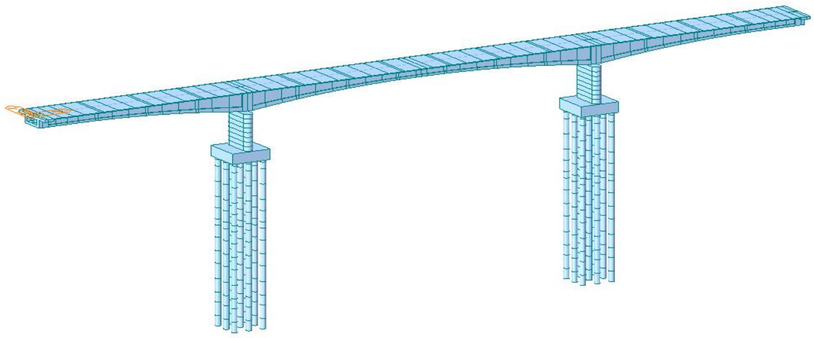

Fig. 2. The bridge superstructure model

3. ElasticTime-History Analysis

The seismic intensity of this bridge site area is 8 degrees. The unfavorable combination of vertical seismic effects and horizontal effects should be considered, while inputting one group of seismic motion time histories of three directional components. In order to consider the randomness of ground motion, the design acceleration time-history must not be less than three groups, and the absolute value of the correlation coefficient ρ between any two groups of time-history in the same direction is less than 0.1.

The above time history excitations are applied to the bridge structure in the longitudinal direction and across the direction respectively, and four load cases are defined. Preliminary seismic verification of the bottom of No.12 pier is conducted in Table 1. After comparison, the extreme values of the elastic time history analysis results are selected as the seismic response, and the anti-seismic capacity is based on the bending moment-curvature of section analysis results. The pier remains elastic under the E1 action, and also elastic in the transverse direction under the E2 action, but plastic hinges appear in the longitudinal direction. Subsequent elasto-plastic time history analysis confirms the results of the preliminary determination of the bridge's seismic state.

Table 1. Seismic verification of piers

Seismic response	E1 Action	E2 Action
Longitudinal MY(MN·m)	104.0<135.3 The piers are elastic, concrete cover is cracked	402.8>160.8 Greater than the ultimate bending moment, plastic hinges appear, the bending moment is not correct, and Elasto-plastic time history analysis is required
Transverse MZ(MN·m)	93.5<172.4 The piers are elastic and the concrete cover is not cracked	311.7<367.7 The piers are elastic, and concrete cover is cracked

ISSN:3007-9640 DOI: https://doi.org/10.70114/acmsr.2025.3.1.P126

4. Elasto-Plastic Time History Seismic Analysis

4.1 Elasto-Plastic Constitutive Relationship

Transverse stirrups can effectively restrain the lateral expansion of concrete, improving the stress-strain relationship of core concrete, preventing longitudinal reinforcement buckling, and enhancing the ductility of reinforced concrete bridge piers. To address this, scholars have proposed concrete models such as the Kent & Park model and the Mander model.

Common models for threaded steel include the Menegotto-Pinto model, the bilinear model, and the trilinear model. Research results indicate that the Menegotto-Pinto model is highly efficient in analysis and fits well with experimental data.

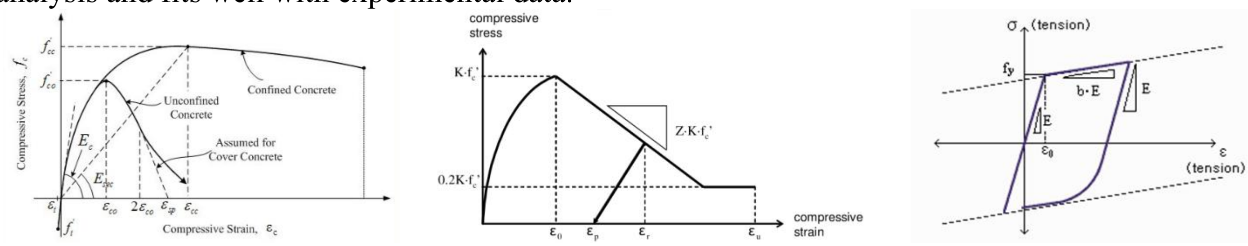

(a) Mander model (b) Kent & Park model (b) Menegotto-Pinto model

Fig. 3. Constitutive model

4.2 Section Bending Moment-Curvature (M-Φ) Analysis

In elasto-plastic seismic analysis, the nonlinear hysteretic characteristics of the section are often used. The nonlinear hysteretic characteristics of the beam and column sections can be described by the bending moment-curvature curve or the load-displacement curve of the section. Therefore, before conducting the elasto-plastic time history analysis, the bending moment-curvature analysis of the pier section is first performed to obtain the first seismic capacity: the seismic performance of the section.

Using the section shape and rebar arrangement to obtain the bending moment-curvature curve of the section and using this curve to evaluate the seismic performance of sections save time for analysis.

For single column pier, the increase or decrease in axial force caused by earthquakes can be neglected. In MIDAS software, Kent & Park Model is used for the material constitutive model of concrete, and Menegotto-Pinto Model is used for the rebar. In UCfyber software, Mander Model is used for the material constitutive model of concrete, and Menegotto-Pinto Model is used for the rebar.

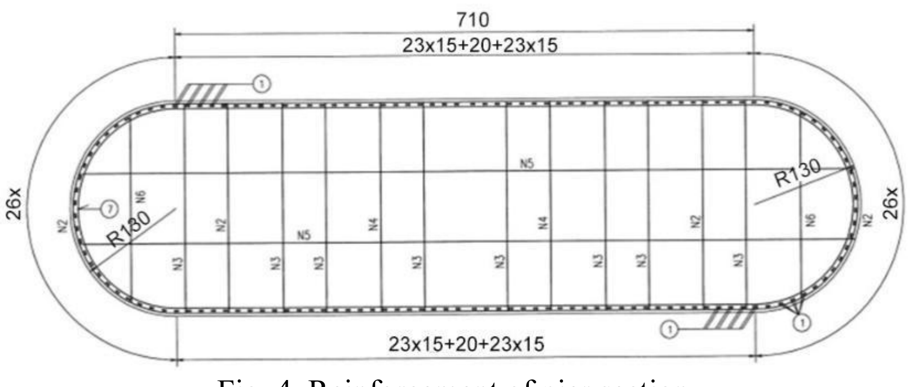

Fig. 4. Reinforcement of pier section

Table 2 compares characteristic points of the M-Φ curve. In the initial yield and equivalent yield states, the two calculation results are relatively close; but in the limit state, there is the significant difference, which should be due to the difference in the constitutive relationship of concrete.

ISSN:3007-9640 DOI: https://doi.org/10.70114/acmsr.2025.3.1.P126

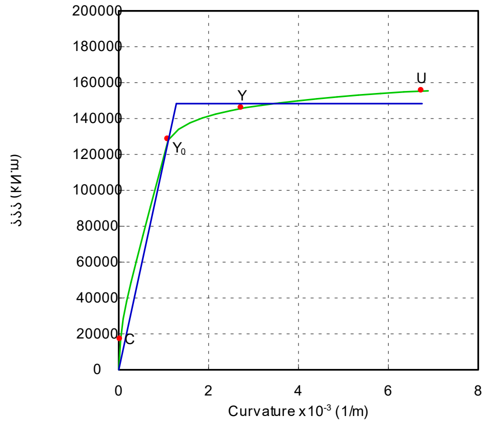

(a) My-Φ

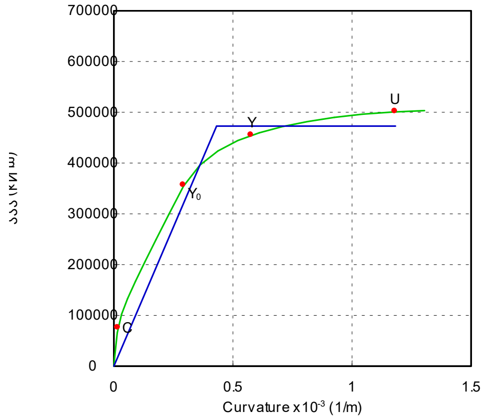

(b) Mz-Φ

Fig. 5. Moment-curvature curve

Table 2. Analysis results of pier bottom section

Software	State	Point	My-Moment (MN·m)	My-Curvature (10^{-3}/m)	Mz-Moment (MN·m)	Mz-Curvature (10^{-3}/m)	Software
Midas	Crack	c	19.3	0.038	172.4	0.066	Crack
	Yield (Initial)	Ys	135.3	1.075	394.5	0.287	Yield (Initial)
	Yield	Y	158.3	3.174	509.5	0.654	Yield
	Yield (Ideal.)	Yeq	160.8	1.278	523.1	0.423	Yield (Ideal.)
	Ultimate	u	169.4	7.602	553.8	1.348	Ultimate
UCfyber	Crack	c	/	/	/	/	Crack
	Yield (Initial)	Ys	137.9	1.111	382.8	0.294	Yield (Initial)
	Yield (Ideal.)	Yeq	160.3	1.291	536.9	0.412	Yield (Ideal.)
	Ultimate	u	207.7	47.00	625.2	8.639	Ultimate

4.3 Results and Discussion

4.3.1 plastic hinge

The D/D1 ductility coefficient is the current deformation divided by the first yield deformation, and the D/D2 ductility coefficient is the current deformation divided by the second yield deformation. Tables 3 and 4 respectively provide the ductility calculation results of Pier No.12 in the longitudinal and transverse directions.

Table 3. Bending ductility results at pier bottom in the longitudinal direction of bridge

Seismic wave	Time (s)	My (MN·m)	Plastic rotation angle ($\times10^{-3}$ rad)	D/D1	D/D2	Yield state	Yield point P1 (MN·m)	Yield point D1 ($\times10^{-3}$ rad)	Yield point P2 (MN·m)	Yield point D2 ($\times10^{-3}$ rad)
1	15.34	89.98	4.856	15.18	0.44	1st yielding	185.7	0.320	290.8	11.11
2	8.22	101.94	5.948	18.59	0.54	1st yielding	185.7	0.320	290.8	11.11
3	46.02	85.37	4.435	13.86	0.40	1st yielding	185.7	0.320	290.8	11.11

ISSN:3007-9640 DOI: https://doi.org/10.70114/acmsr.2025.3.1.P126

Table 4. Bending ductility results at pier bottom in the transverse direction of bridge

Seismic wave	Time (s)	My (MN·m)	Plastic rotation angle ($\times10^{-3}$ rad)	D/D1	D/D2	Yield state	Yield point P1 (MN·m)	Yield point D1 ($\times10^{-3}$ rad)	Yield point P2 (MN·m)	Yield point D2 ($\times10^{-3}$ rad)
1	17.22	261.4	0.485	4.70	0.35	1st yielding	655.1	0.103	1057.5	1.401
2	34.70	260.7	0.483	4.68	0.34	1st yielding	655.1	0.103	1057.5	1.401
3	24.36	260.9	0.483	4.69	0.34	1st yielding	655.1	0.103	1057.5	1.401

Under E2 action, plastic hinges appear on the piers in the longitudinal direction, and the bending moment My cannot truly reflect the structure internal force. By using displacement value, the plastic rotation angle of the bottom of the pier reaches 5.948×10-3rad, the ductility coefficient of the pier top displacement is D/D1=18.59, and it is in the first yield state. Small plastic hinges also appeared on the piers in the transverse direction, and the plastic rotation angle of the pier bottom reached 0.485×10-3rad, and the displacement ductility coefficient of the pier top is D/D1=4.70.

Figure 6 shows the calculation results of Pier No.12 under the action of the first group of seismic waves, where (a) represents the longitudinal bending moment My, (b) represents the plastic rotation angle, (c) represents the ductility coefficient D/D1, and (d) indicates that the pier has exceeded the first yield state and entered the second yield state.

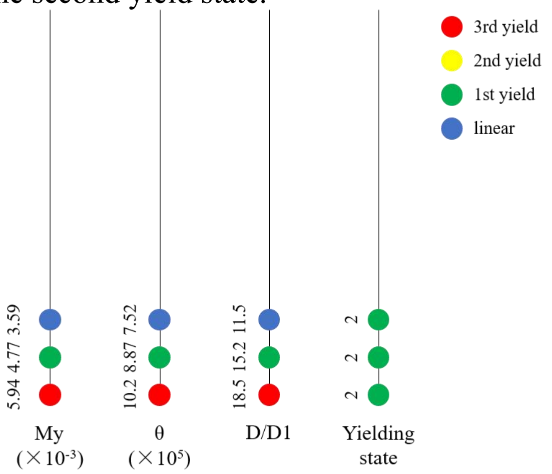

Fig. 6. Moment-curvature curve (My-Φ and Mz-Φ)

Figure 7 show the curve of the bending moment at the bottom of the pier with time.

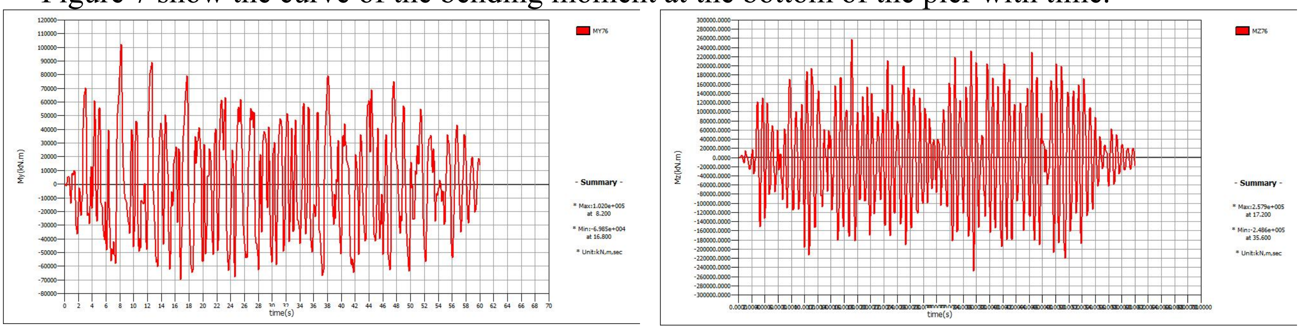

(a) My (b) Mz

Fig. 7. Curve of the bending moment at the bottom of the pier with time

Looking at the hysteretic curve of the bending moment-rotation angle in the potential plastic hinge area at the pier bottom, Figure 8 shows that the pier (red line) enters full bending plasticity in the longitudinal direction of bridge, the skeleton curve is a parallelogram; the transverse bending of

ISSN:3007-9640 DOI: https://doi.org/10.70114/acmsr.2025.3.1.P126
the pier (green line) remains a small amount of plasticity, the skeleton curve is distributed in the narrow area, which can be regarded elastic.

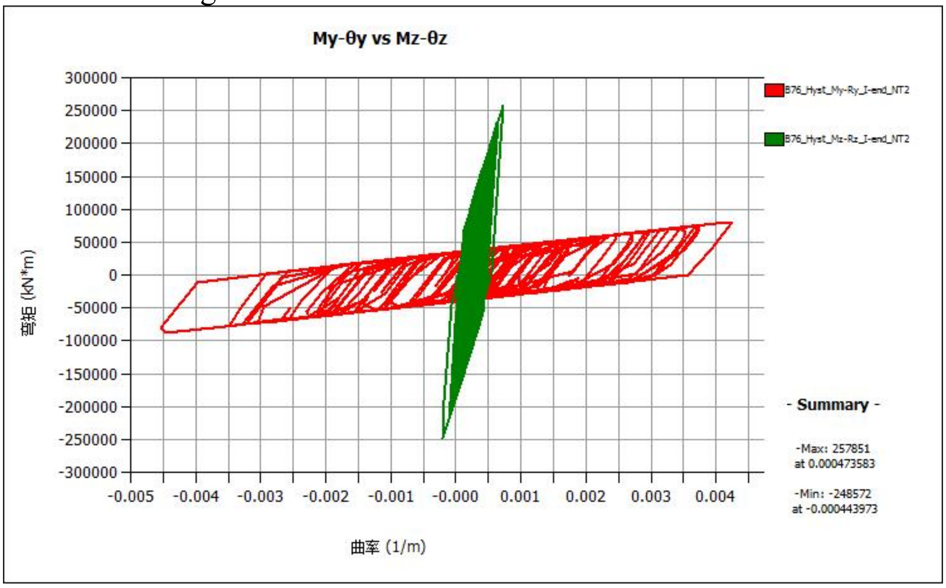

Fig. 8. Hysteretic curve of the bending moment-rotation angle at the pier bottom

4.3.2 Displacement verification at pier top

Checking the hysteresis curve of the bending moment in the potential plastic hinge area at the pier bottom and the displacement at the pier top. Figure 9 shows that the pier enters bending plasticity in the longitudinal direction of bridge. The bending moment My of the pier bottom in the longitudinal direction is the range from 102MN.m to -70MN.m. The displacement of the pier top is the range from -68mm to 136mm, which exceeds the allowable displacement (73-98mm) of the pier top and does not meet the seismic code requirements.

The pier enters small area of bending plasticity in the transverse direction. The bending moment My of the pier bottom in the longitudinal direction is the range from 258MN.m to -249MN.m, and the displacement of the pier top is the range from -37 mm to 39mm, which exceeds the allowable displacement of 23mm at the pier top, which does not meet the seismic code requirements.

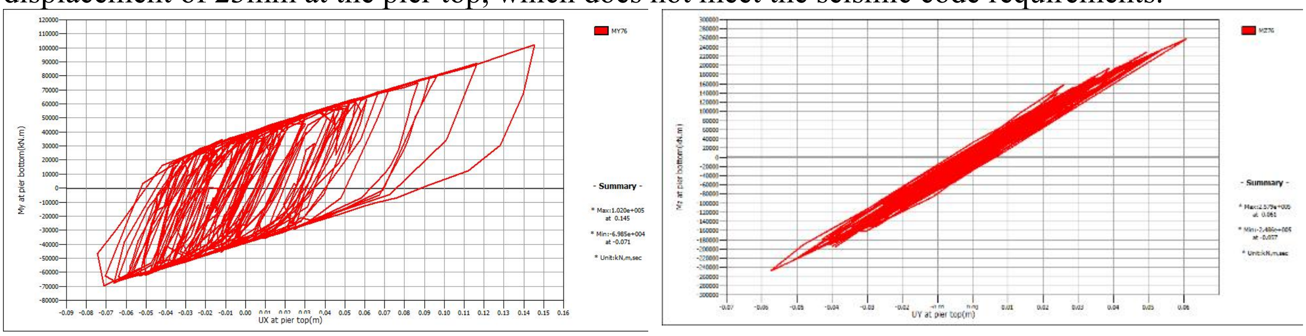

(a) My-Ux (b) Mz-Uy

Fig. 9. Hysteresis curve of bending moment at pier bottom and displacement at pier top

5. Summary

By using the elastic time-history analysis and elasto-plastic time history analysis, the seismic response of the bridge is calculated step by step. Through the bending moment-curvature analysis of the pier section, the pier section resistance and the permissible displacement of the pier top are obtained. Analysis conclusions are as follows:

(1) The seismic state of piers can be easily determined through response spectrum and elastic time history methods.

ISSN:3007-9640 DOI: https://doi.org/10.70114/acmsr.2025.3.1.P126

(2) Using a plastic hinge model to simulate piers, under E2 action, the piers enter a bending plastic state in the longitudinal direction, which is in the first yield state. There is a slight plastic state in the transverse bending of the pier.

References

[1] Abbas H H, Sause R, Driver R G. Analysis of flange transverse bending of corrugated web I-girders under in-plane loads. Journal of Structural Engineering-Asce, 2007, 133(3): 347-355.

[2] Ding Yong., Jiang KeBin., Liu YaWen. Nonlinear analysis for PC box-girder with corrugated steel webs under pure torsion. Thin-Walled Structures, 2012, 51: 167-173.

[3] Li Hongjiang. Shear Behavior of Prestressed Concrete Box Girders with Corrugated Steel Webs: An Overview. Nanjing, PEOPLES R CHINA, 2019; pp. 181-191.

[4] Moon J, Ko H, Sung H I, et al. Natural Frequency of a composite girder with corrugated steel web. Steel and Composite structures,2015,18(1):255-271.

[5] Hongyi Wei, Zhiqiang Wang, Qinghai Feng. Seismic Analysis and Design of Minpu Double-deck Cable Stayed Bridge. Procedia Engineering, 2011, 14: 1501-1509.

[6] Bathe K., Finite element procedures. 2006.

[7] Suzuki J , Zayernouri M ,Bittencourt M , et al. Fractional-order uniaxial visco-elasto-plastic models for structural analysis[J]. Computer Methods in Applied Mechanics and Engineering, 2016, 308: 443-467.

[8] Zhao Nan, Ma Kai, Tang Shaoxue, Chen Binlei and Li Ting, Elastoplastic time-history analysis on multi-tower isolated structure with an enlarged base[J/OL]. 2011.